

Original Paper

# Htra1 is a Novel Transcriptional Target of RUNX2 That Promotes Osteogenic Differentiation

Paul P.R. Iyyanar<sup>a,b</sup> Merlin P. Thangaraj<sup>a</sup> B. Frank Eames<sup>c</sup> Adil J. Nazarali<sup>a</sup>

<sup>a</sup>Laboratory of Molecular Cell Biology, College of Pharmacy and Nutrition and Neuroscience Research Cluster, University of Saskatchewan, Saskatoon, SK, Canada, <sup>b</sup>Division of Developmental Biology, Cincinnati Children's Hospital Medical Center, Cincinnati, OH, USA, <sup>c</sup>Department of Anatomy and Cell Biology, University of Saskatchewan, Saskatoon, SK, Canada

## Key Words

Runx2 • Htra1 • Osteoblast differentiation • Matrix mineralization

## Abstract

**Background/Aims:** *Runt-related transcription factor 2 (Runx2)* is a master regulator of osteogenic differentiation, but most of the direct downstream targets of RUNX2 during osteogenesis are unknown. Likewise, High-temperature requirement factor A1 (HTRA1) is a serine protease expressed in bone, yet the role of *Htra1* during osteoblast differentiation remains elusive. We investigated the role of *Htra1* in osteogenic differentiation and the transcriptional regulation of *Htra1* by RUNX2 in primary mouse mesenchymal progenitor cells. **Methods:** Overexpression of *Htra1* was carried out in primary mouse mesenchymal progenitor cells to evaluate the extent of osteoblast differentiation. Streptavidin agarose pulldown assay, chromatin immunoprecipitation assay, and dual luciferase assay were carried out to investigate the interaction of RUNX2 protein at the *Htra1* promoter during osteoblast differentiation. **Results:** Overexpression of *Htra1* increased the production of mineralized bone matrix, upregulating several osteoblast genes, such as *Sp7 transcription factor (Sp7)* and *Alkaline phosphatase, liver/bone/kidney (Alpl)*. In addition, *Htra1* upregulated osteogenesis-related signalling genes, such as *Fibroblast growth factor 9 (Fgf9)* and *Vascular endothelial growth factor A (Vegfa)*. A series of experiments confirmed *Htra1* as a direct RUNX2 transcriptional target. Overexpression of *Runx2* resulted in the upregulation of *Htra1* mRNA and protein. Chromatin immunoprecipitation and streptavidin agarose pull-down assays showed that RUNX2 binds a proximal -400 bp region of the *Htra1* promoter during osteogenic differentiation. Dual luciferase assays confirmed that RUNX2 activates the proximal *Htra1* promoter during osteogenic differentiation. Mutation of putative RUNX2 binding sites revealed that RUNX2 interacts with the *Htra1* promoter at -252 bp and -84 bp to induce *Htra1*

expression. **Conclusion:** We demonstrate that *Htra1* is a positive regulator of osteogenic differentiation, showing for the first time that *Htra1* is a direct downstream target of RUNX2.

© 2019 The Author(s). Published by  
Cell Physiol Biochem Press GmbH&Co. KG

## Introduction

RUNX2 is a master regulatory transcription factor critical for osteogenic differentiation and bone formation [1]. *Runx2* null mutant mice exhibit neonatal lethality with complete lack of ossification [1], and *RUNX2* haploinsufficiency in humans results in cleidocranial dysplasia, a skeletal disorder characterized by bone and dental abnormalities [2–4]. RUNX2 regulates several osteogenic genes, such as *Integrin binding sialoprotein (Ibsp)* [5], Matrix metalloproteinase-13 (*Mmp13*) [6, 7], and *Sp7* [8, 9], by binding a consensus site RCCRC(A/T) [10] in their proximal promoter regions. However, a likely majority of the transcriptional targets of RUNX2 during osteogenic differentiation remain to be characterized [11].

HTRA1 is one of four members of the HTRA family of serine proteases. HTRA1 has been implicated in several diseases, including age-related macular degeneration [12], cerebral autosomal recessive arteriopathy with subcortical infarcts and leukoencephalopathy (CARASIL) [13–15], and cancer [16, 17]. HTRA1 is expressed in hypertrophic chondrocytes and osteoblasts under both physiological [18] and pathological conditions, including osteoarthritis [19] and the fracture callus [20]. Despite *Htra1* expression in bone, published studies conflict in concluding whether *Htra1* is a positive or negative regulator of osteogenesis. Some studies have demonstrated that *Htra1* is an inducer of osteogenic differentiation, where it is involved in the lineage commitment of mesenchymal stem cells to form osteoblasts [20] at the expense of adipocytes [21]. Silencing *Htra1* abolishes osteogenic differentiation induced by all-*trans* retinoic acid in adipose-derived stromal cells [22]. In contrast, other studies have found *Htra1* to be a negative regulator of osteogenesis in 2T3 osteoblasts [23] and the KusaO cell line [24]. Therefore, the role of *Htra1* in osteogenesis remains unclear.

Very little information is available on the gene networks and signalling pathways downstream of *Htra1* in osteogenic differentiation. HTRA1 has proteolytic activity, degrading various substrates in the extracellular matrix (ECM), such as Fibronectin, Fibulin, and Nidogen [15, 25–27]. In *Xenopus* embryos, *Htra1* shares similar expression domains with FGF ligands, such as FGF8 and FGF4, and *Htra1* promotes long-range FGF signalling via cleavage of proteoglycans, such as Biglycan, Syndecan-4, and Glypican-4 [28]. Such an impact of *Htra1* on FGF signalling could influence bone formation. *Fgf9* induces *Vegfa* expression for skeletal vascularization of the proximal limb during development [29]. Furthermore, FGF9 promotes *Vegfa*-mediated *Mmp9* expression for the bone remodelling process in the long bones [30]. FGF8 also induces *Htra1* in developing chick facial mesenchyme [31], suggesting reciprocal feedback. *Htra1* promotes ERK/MAPK-dependent MMP expression during adipogenic differentiation, potentially via breakdown of ECM-related components such as Fibronectin [21]. In human bone marrow stem cells, HTRA1 suppresses the expression of *Sclerostin (Sost)*, an inhibitor of WNT signalling-dependent osteogenesis [20]. Further insights into the molecular signalling downstream of *Htra1* is necessary to decipher its role in osteogenesis.

Mesenchymal progenitor cells from the embryonic palate differentiate directly into osteoblasts to form the palatal bones through the process of intramembranous ossification [32–34]. In the present study, we have investigated the impact of *Htra1* overexpression on the expression of osteogenic markers and matrix mineralization during osteogenic differentiation of primary palatal mesenchymal progenitor cells *in vitro*. Furthermore, we examined the transcriptional regulation of *Htra1* by RUNX2 during osteogenic differentiation. Data reveal that *Htra1* is a positive modulator of osteogenic differentiation, regulating the expression of several key osteogenic genes. In addition, our data demonstrate for the first time that RUNX2 binding to the proximal *Htra1* promoter is necessary and sufficient to induce *Htra1* expression, thus elucidating *Htra1* as a novel direct downstream target of RUNX2 that promotes osteogenesis.

## Materials and Methods

### *Immunohistochemistry*

Immunohistochemistry was carried out as previously described [34]. Briefly, mouse embryonic heads of stage E16.5 were fixed with freshly prepared 4% paraformaldehyde overnight and rehydrated in 30% sucrose at 4°C. Frozen coronal sections (10 µm) were rehydrated with PBS for 45 min, permeabilized with 0.1% Triton X-100 and blocked with 3% skim milk containing 0.1% Triton X-100 in 1X PBS for 1 h at room temperature. Sections were then incubated overnight with the following primary antibodies: HTRA1 (1:200; Abcam ab38611), RUNX2 (1:200; Abcam ab23981) or SP7 (1:800; Abcam ab22552) in 1X PBS with 0.1% Triton X-100 at 4°C. Sections were washed three times and treated with secondary antibodies conjugated with Alexa Fluor® 594 (1:400; Invitrogen) in 1X PBS with 0.1% Triton X-100 at room temperature for 1.5 h. Stainings with rabbit IgG served as a negative control to assess specific staining of primary antibodies employed in the study. Sections were then washed three times, five mins each and mounted in Prolong gold antifade reagent (Invitrogen) for imaging.

### *Primary mesenchymal progenitor cells derived from mouse embryonic palate*

Primary mesenchymal progenitor cells were isolated from the palatal shelves of wild-type C57BL/6J mouse embryos at embryonic day (E)13.5 as previously described [34, 35]. Briefly, palatal shelves were micro-dissected from the maxilla of E13.5 embryos and incubated with 0.25% trypsin (Sigma) for 15 min at 37°C [36]. Cells were gently pipetted up and down, passed through 70-µm-cell strainer (BD Falcon) and plated on poly-D-lysine-coated T25 flasks. Cells were cultured in Dulbecco's Modified Eagle's Medium (DMEM): Ham's F12 (DMEM/F12) (1:1) media containing 10% FBS, 1% antibiotic-antimycotic solution (Sigma) and passaged no more than three times. Osteogenic differentiation was induced as described previously [34, 37] with minor modifications. Briefly, mesenchymal progenitor cells were seeded on PDL-coated 24-well plates at a cell density of  $5 \times 10^4$  cells per well in triplicate and cultured until they reach confluence. Osteogenic differentiation was induced with osteogenic differentiation medium comprising of DMEM with 4, 500 mg/L glucose, 10% FBS, 2mM L-glutamine, 1% antibiotic-antimycotic solution, 50µg/ml L-ascorbic acid 2-phosphate sesquimagnesium salt (Sigma), 10 mM β-glycerophosphate (Sigma) and 100 nM dexamethasone (Sigma). Media was changed every third day for up to 8, 14 or 21 days. Cells were harvested for RNA isolation or fixed for alkaline phosphatase (ALP) staining at day 8 and 15.

### *Alkaline phosphatase (ALP) staining*

ALP staining was carried out as previously described [34, 38]. Primary mesenchymal progenitor cells were washed once with PBS (pH 7.4), followed by fixation in 4% paraformaldehyde for 15 min and then washed twice with PBS. Cells were then treated with ALP buffer (100 mM NaCl, 100 mM Tris-HCl pH 9.5, 50 mM MgCl<sub>2</sub>, 0.1% Tween-20) for 10 min prior to staining with 4.5 µl/ml of 5-Bromo-4-chloro-3-indolyl phosphate and 3.5 µl/ml of nitro blue tetrazolium in ALP buffer for 10 min. The reaction was stopped with PBS containing 20 mM EDTA buffer. Images were taken using a bright field microscope and the percentage area of ALP-positive blue staining was quantified using ImageJ (NIH) [39].

### *Alizarin red S (ARS) staining and quantitation*

ARS staining and quantitation was carried out as described [34, 40] with minor modifications. Briefly, primary mesenchymal progenitor cells were washed once with PBS, pH 7.4, followed by fixation in 4% paraformaldehyde for 15 min and then washed two times with PBS. Cells were subsequently washed with deionized water to remove excess PBS, prior to the addition of 250 µl of 40 mM ARS (Sigma) solution (pH 4.1). Cells were incubated at room temperature for 20 min with gentle shaking. Excess dye was aspirated, and cells were washed with deionized water and imaged using bright field microscopy. For quantitation of ARS, 400 µl of 10% acetic acid (Fisher Scientific) was added to each well and incubated for 30 min with shaking. The cells were then dislodged using a cell scraper (Fisher Scientific) and transferred to a microcentrifuge tube containing 10% acetic acid. After vortexing for 30 s, samples were heated at 85°C for 10 min and cooled on ice for 5 min. The slurry was centrifuged at 15,000 g for 15 min and 300 µl of the supernatant transferred to a new micro-centrifuge tube followed by the addition of 150 µl of 10% solution of ammonium hydroxide (Sigma). After vortexing, 150 µl was transferred from this mixture to an opaque walled 96-well plate for measurement of absorbance at 405 nm. A standard plot of ARS concentration was constructed by serially

diluting 40 mM ARS in a buffer containing 10% (v/v) acetic acid and 10% (v/v) ammonium hydroxide. Absorbance values of standard concentrations were used to interpolate concentrations of the test sample.

#### Quantitative real-time polymerase chain reaction (qPCR)

Total RNA was isolated from the mesenchymal progenitor cells using RNA mini spin column as per the manufacturer's protocol (BioRad). First strand cDNA synthesis (Reverse transcription) was performed in 20 µl reactions with 500 ng of total RNA using High-Capacity cDNA Reverse Transcription Kit (Invitrogen). qPCR was carried out using SYBR green master mix (Invitrogen) in 7300-real-time PCR system (Applied Biosystems). The primer pairs used for qPCR are listed in Table 1.

#### Htra1 overexpression transfections

*Htra1* vector (Origene) was digested using *Sall* and *XhoI* restriction enzymes to separate the *Htra1* cDNA, and the empty vector (pCMV6-myc-ddk) was generated by self-ligation of *Sall* and *XhoI* compatible sticky ends. Site-directed mutagenesis of *Htra1* at nucleotides corresponding to serine 328 to alanine; *Htra1* (*mut*) [41] was carried out by PCR using QuikChange Lightning kit (Agilent Technologies) with the following primers: 5'CATCAATTATGGAAATGCCGGAGGCCCGTTAG 3' and 5'GTAGTTAATACCTTACGGCCTCCGGGCAATC 3'. Primary mesenchymal progenitor cells were transfected with polyethylenimine (PEI) (Linear Mol. Wt 25, 000, Polysciences, Inc.). For each well of a 24-well plate, 700 ng of *Htra1*, *Htra1* (*mut*) or empty vector were transfected with 1.5 µl of PEI (1 mg/ml), every third day in antibiotic-free media in the presence of serum. Cells were either fixed for ALP or ARS staining or lysed for RNA isolation at indicated time points. Similarly, the *Runx2* vector (Origene) was transfected as described above for the overexpression of *Runx2* in primary mesenchymal progenitor cells.

#### Osteogenic array

Osteogenesis and bone remodelling real-time PCR array (Bio-Rad), which contains a set of 84 osteogenic pathway related genes in 96-well format, was used to determine differentially regulated genes after overexpression of *Htra1*. Primary mesenchymal progenitor cells were transfected as described above, with *Htra1* or empty vector and allowed to differentiate for seven days. 1000 ng of RNA was converted to cDNA in 20 µl reactions. The cDNA sample was diluted with 100 µl of nuclease-free water and 1 µl of cDNA was used to load each well of the 96-well plate. *Gapdh* was used as an endogenous control and relative gene expression was determined using the  $\Delta\Delta Ct$  method. Three biological replicates each for samples treated with *Htra1* overexpression vector or empty vector were run individually and analyzed together to get the relative gene expression data. Gene expression in *Htra1*-overexpressed samples greater than 1.5-fold was considered upregulated and lesser than 0.6-fold was considered as downregulated, relative to the expression in the empty vector-treated samples.

**Table 1.** Primer sequences used for the relative quantitation of transcripts in primary mesenchymal progenitor cells by qPCR using SYBR green assay

Transcript	Primer sequences	Length (bases)	Amplicon size (bp)
Alkaline phosphatase, liver/bone/kidney (Alpl)	CCTTGACTGTGGTTACTGCT	20	216
	CCTGGTAGTTGTTGTGAGCG	20	
High temperature requirement factor A1 (Htra1)	AGTTCTTGACAGAGTCCCACGA	22	154
	TATGCCCCAGAGACACATCC	21	
Runt-related transcription factor 2 (Runx2)	TGCCTCCGCTGTTATGAAAA	20	187
	CTGTCTGTGCCTTCTTGGTT	20	
Sp7 transcription factor (Sp7)	CACAAAGAAGCCATACGCTG	20	165
	CCAGGAAATGAGTGAGGGAAG	21	
18s ribosomal RNA (18s rRNA)	CGCGGTTCTATTTTGTGGT	20	219
	AGTCGGCATCGTTTATGGTC	20	

### *Biotinylated probes*

Biotinylated probes were synthesized by PCR amplification from mouse genomic DNA using 5' biotin-labeled primers (Invitrogen). The primer pairs used for the synthesis of 1 kb *Htra1* promoter probe (-994 to +72 bp) were forward 5'-biotin-TCCTCCTTGAGTCAGGGTCA-3' and reverse 5'-biotin-GCAGCAGTAGCAAAGACAGG-3'. The primers for the -400 bp probe were forward primer 5'-biotin-AAGTTCACAGCCACAGTCCC-3' and reverse primer 5'-biotin-TAGCAAAGACAGGAGCGTGG-3'. The annealing temperature for the primers was 60°C. All PCR amplified biotinylated probes were electrophoresed on an agarose gel and purified using a gel extraction kit (Thermo Fisher).

### *Streptavidin agarose pull-down assay (SAPA)*

SAPA was carried out as previously described [42, 43] with minor modifications. Primary mesenchymal cells were harvested 5 days after differentiation and lysed with RIPA buffer containing 50 mM Tris-HCl, pH 7.4, 1% NP-40, 0.25% sodium deoxycholate, 150 mM NaCl, 1 mM NaF, 1 mM Na<sub>3</sub>VO<sub>4</sub>, 1 mM EDTA, and 1% protease inhibitor cocktail (Sigma). Lysates were vortexed, passed through a 28-gauge needle, incubated on ice for a minimum of 30 min, and centrifuged. Protein concentration in the supernatant was measured using the Bradford assay. SAPA was carried out using 5 µg biotinylated DNA probe added to the cell lysates (250 µg) and incubated at 4°C overnight with rotational mixing. Streptavidin-agarose beads (20 µl) were added to each sample and incubated for 4 h at 4°C with rotation. The beads were then washed four times with 1 ml RIPA buffer and centrifuged at 4°C. Beads were then suspended in 30 µl of 2X SDS loading buffer, boiled for 15 min and centrifuged. The resulting supernatant was used for western blot analysis.

### *Western blot analyses*

Western blot analyses were carried out as previously described [34]. Briefly, proteins separated on a 12% sodium dodecyl sulfate (SDS)-polyacrylamide gel and blotted to PVDF membranes (Bio-Rad) for 2 hours at 4°C. Blots were blocked with 4% skimmed milk for 1 hour and incubated with primary antibody anti-RUNX2 rabbit polyclonal (1:500; Cell signaling D1H7), anti-HTRA1 rabbit polyclonal (1:1000; Abcam 38611) and β-actin mouse monoclonal (1:3000; Cell Signaling) overnight at 4°C. Anti-rabbit IgG HRP-conjugate (Bio-Rad) (1:3000) secondary antibody was incubated for 1 hour at room temperature. Bands were visualized with Clarity™ Western ECL Substrate (BioRad) and imaged using CCD-camera in Syngene imaging system.

### *Chromatin immunoprecipitation assay*

Chromatin immunoprecipitation (ChIP) assay was carried out [43] using a rabbit monoclonal antibody against RUNX2 (Cell Signaling D1H7). Briefly, mesenchymal cells were cross-linked with 0.75% formaldehyde in 1x PBS for 10 min and were lysed with cell lysis buffer containing 50mM HEPES-KOH (pH 7.5), 140mM NaCl, 1mM EDTA (pH 8), 1% Triton X-100, 0.1% sodium deoxycholate, 0.1% SDS and 1% protease inhibitors. Samples were then sonicated to shear the DNA with four rounds of 12 sec pulses each at 50% power output and 90% duty cycle using a Branson Sonicator 200. 50 µg of sonicated DNA was suspended in 1 ml of ChIP dilution buffer containing 1% Triton X-100, 2mM EDTA (pH 8), 20mM Tris-HCl (pH 8), 150mM NaCl, and 1% protease inhibitors for each immunoprecipitation. The precleared samples were then mixed with either the RUNX2 monoclonal antibody or normal rabbit IgG and rotated at 4°C overnight. This was followed by the addition of 40 µl of protein A/G beads to the immunoprecipitated complex and further mixing by rotation at 4°C for 4 h. Beads were then washed four times with low salt wash buffer containing 0.1% SDS, 1% Triton X-100, 2mM EDTA (pH 8), 20mM Tris-HCl (pH 8), and 150mM NaCl and two times with high salt buffer containing 0.1% SDS, 1% Triton X-100, 2mM EDTA (pH 8), 20mM Tris-HCl (pH 8), and 500 mM NaCl at 4°C for 2 min each. The immunoprecipitated complex was eluted using elution buffer containing 1% SDS and 100mM sodium bicarbonate at 30°C for 15 min. The eluted DNA samples were treated with proteinase K (10 µg/ml) and RNase A (20 µg/ml) and incubated at 65°C for 2 h. Following incubation, DNA concentration was measured, and PCR was carried out using the primer set to amplify -295 to +72 bp region of the *Htra1* promoter.

#### Cloning of Htra1 promoter regions

Five different regions of the 1 kb *Htra1* promoter were amplified by PCR using Phusion High-Fidelity DNA polymerase (NEB) with the primers listed in Table 2. Using dATP, an A-overhang was introduced to the 3' end of the PCR amplicons by non-proof reading Taq DNA polymerase (Lucigen). The PCR products were then purified by gel extraction and cloned into the pGEM-T easy vector (Promega). From the positive clones, the respective *Htra1* promoter fragments were digested with *KpnI* and *XhoI* for cloning into the destination pGL3 promoter luciferase vector (Promega). All clones were verified by Sanger sequencing at National Research Council (NRC) sequencing facility (Saskatoon, SK, Canada) and found to match perfectly with the promoter region of *Htra1* (*M. musculus*[chr7]138078749-138079949). Three RUNX2 putative binding sites in the 0.4 kb *Htra1* promoter (-399 to +72) at -252 bp (Mut1), -84 bp (Mut2) and +11 bp (Mut3) were mutated alone or in combination using QuikChange Lightning kit (Agilent Technologies) with the primer pairs listed in Table 2.

#### Luciferase assay

Dual luciferase reporter assay (Promega) was carried out as previously described [44]. Briefly,  $1 \times 10^4$  primary mesenchymal progenitor cells were seeded into the white opaque 96-well plate. The cells were transfected with 100 ng of pGL3 firefly luciferase vector containing different fragments of the *Htra1* promoter constructs, 100 ng of either the empty vector (pCMV6-myc-ddk) or the *Runx2* expression vector; 40 ng of pRL-CMV *Renilla* luciferase vector was used as the transfection control. After 48 h, cells were lysed with the passive lysis buffer and then firefly luciferase assay reagent II was added to measure the firefly luciferase activity. This was followed by the addition of Stop & Glo reagent and the *Renilla* luciferase activity was measured. The relative luciferase activity was calculated by normalizing the firefly luciferase activity values to the respective *Renilla* luciferase values.

#### Statistical analyses

Statistical analyses were carried out using unpaired two-tailed T-test in the case of two groups. One-way ANOVA with Bonferroni multiple comparison test was used to analyze data with more than two groups, two-way ANOVA was carried out to analyze data with two variables in the study and a p-value of <0.05 was considered significant. Analyses are from at least three independent experiments and the respective number of biological replicates are mentioned in the figure legends.

**Table 2.** Primer sequences used for cloning of Htra1 promoter fragments into pGL3 promoter luciferase vector. The underlined sequences denote restriction sites for KpnI and XhoI, which were used to clone Htra1 promoter fragments into the destination vector. Sequences in bold are the mutated putative RUNX2 binding sites

Htra1 promoter region	Primer sequences
-994 to +72 bp	TAGGTACCTCCTTGAGTCAGGGTCA TACTCGAGTAGCAAAGACAGGAGCGTGG
-399 to +72 bp	TAGGTACCAAGTTCACAGCCACAGTCC TACTCGAGTAGCAAAGACAGGAGCGTGG
-811 to -439 bp	TAGGTACCGGTGACAGTTGCTCTTCTCTGA ATCTCGAGAAACCCAGTGCCAGACCTA
-295 to +72 bp	AAGGTACCTTTCCAGGCGATTGCGCAGT TACTCGAGTAGCAAAGACAGGAGCGTGG
-199 to +72 bp	CCGGTACCGGTCTTCAATCTCTGAGGAAA TACTCGAGTAGCAAAGACAGGAGCGTGG
Mut1	GATTGAAGACCTTAAGACCAAATA <b>AT</b> ACGTAACAGAGGGAAACCTGCCTAGCACTGCCG CGGCAGTGCTAGGCAGGTTTCCCTCTGTTACGT <b>ATTATTTT</b> GGTCTTAAGGTCTTCAATC
Mut2	GGTTAAGCCATTGGCCTAACA <b>CAAT</b> GACGAAGCGCCAGGGGGA TCCCCCTGGCGCTTCGTCAT <b>TGTTGTT</b> AGGCCAATGGGCTTAACC
Mut3	CGGCCACGGGCTGG <b>ATTATAGAT</b> GAAAAACCGCCTCGGGA TCCCGAGCGCGGTTTTC <b>ATCTATAAT</b> CCAGCCCGTGCCG

## Results

### *HTRA1 is expressed in developing bones*

To establish a relationship between *Htra1* and developing mouse craniofacial bones, the spatial expression of the HTRA1 protein was examined using immunohistochemistry (IHC). IHC staining revealed that HTRA1 was mainly expressed in ossifying regions of the maxilla and mandible in wild-type embryos at E16.5 (Fig. 1A, E). Osteoblast markers RUNX2 and SP7 (formerly called OSX) exhibited similar expression patterns as HTRA1 in the developing maxilla (Fig. 1B, C) and mandible (Fig. 1F, G) region. Negative control IgG staining revealed the specificity of the HTRA1, RUNX2 and SP7 antibodies (Fig. 1D, H). The expression pattern of HTRA1 in ossifying craniofacial regions of the mouse embryo suggests that *Htra1* might play a role in osteoblast differentiation of primary progenitor cells of craniofacial mesenchyme.

### *Htra1 promotes mineralized matrix production and osteogenic gene expression in primary mesenchymal progenitor cells*

To test the nature of the primary mesenchymal progenitor cells to form mature osteoblasts, we subjected these cells to osteogenic differentiation for up to 21 days and assessed matrix mineralization using ARS staining at day 15 and day 21. Mesenchymal progenitor cells grown in growth media did not develop any mineralized nodules at day 15 or day 21 (Supplementary Fig. 1A, B – for all supplemental material see [www.cellphysiolbiochem.com](http://www.cellphysiolbiochem.com)), while cells differentiated with osteogenic media exhibited matrix deposition and mineralization at day 15 and day 21 (Supplementary Fig. 1C, D). To investigate if *Htra1* plays a role in osteoblast differentiation, we overexpressed *Htra1* in primary mesenchymal progenitor cells for up to 21 days. A vector containing an inactive proteolytic mutant of *Htra1* (*Htra1* (*mut*)) [41] generated by site-directed mutagenesis and an empty vector were used as controls. At day (d)8, ALP staining did not reveal a considerable difference among primary mesenchymal progenitor cells transfected with either the empty vector, the *Htra1* vector, or the *Htra1* (*mut*) vector (Fig. 2A, B, C and M). However, overexpression of *Htra1* resulted in a clear increase in ALP staining at d15, compared to the empty vector- and *Htra1* (*mut*)-transfected cells (Fig. 2D, E, F and N). In addition, ARS staining reflected increased mineralized matrix in *Htra1*-overexpressed cells, compared to cells treated with empty vector and *Htra1* (*mut*) at both d15 (Fig. 2G, H, I) and d21 (Fig. 2J, K, L). Quantitation of the ARS-bound matrix

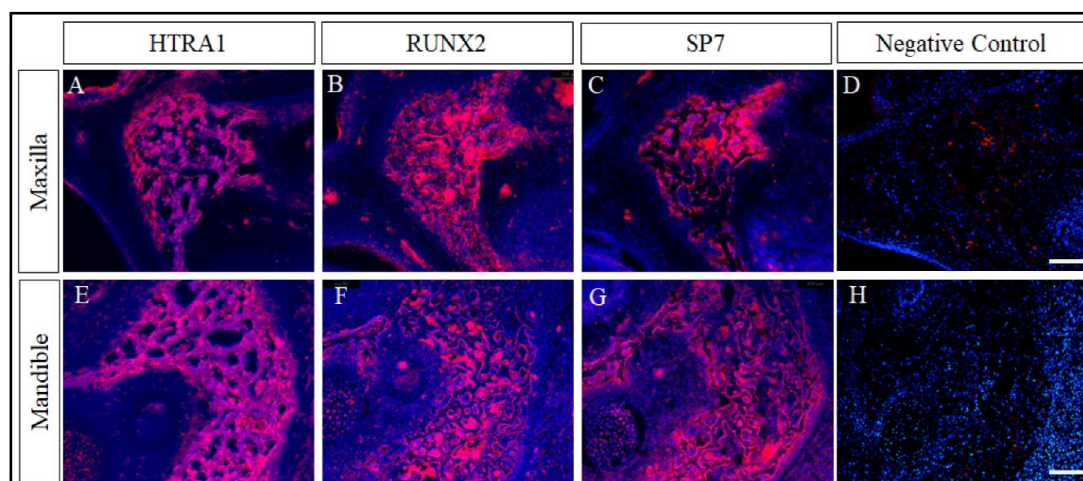


**Fig. 1.** HTRA1 is expressed in the craniofacial bone regions of the developing embryos. Immunohistochemical (IHC) staining of HTRA1 in craniofacial regions of wild-type embryonic heads at E16.5. HTRA1 is expressed predominantly in the developing bones of the maxilla (A) and mandible (E) regions. IHC staining of RUNX2 (B and F), SP7 (C and G) and negative control IgG (D and H) of similar regions from adjacent sections in wild-type embryos at E16.5. Scale bars=200µm.

revealed a significant increase in the amount of bone matrix in *Htra1*-overexpressed cells at d15 and d21, compared to both empty vector- and *Htra1 (mut)*-transfected cells (Fig. 2O, P). In fact, the *Htra1 (mut)*-transfected cells produced levels of mineralized matrix that were indistinguishable from empty vector-transfected cells. These results demonstrate that *Htra1* can increase the production of mineralized bone matrix in primary mesenchymal progenitor cells, and that *Htra1* function in this process could be inhibited by mutating the protease domain.

To elucidate a potential signalling pathway stimulated by *Htra1* during osteoblast differentiation of mesenchymal progenitor cells, *Htra1*-responsive genes were identified using an ossification and bone remodelling real-time PCR array. Several genes, such as *Fgf9*, *Ibsp*, *Vegfa*, *Col2a1*, and *Mmp9*, were upregulated significantly by 1.98, 2.97, 1.52, 2.33, and 4.04-fold, respectively, in *Htra1*-overexpressed cells at d7, compared to empty vector-transfected cells (Fig. 3A). Additional osteogenesis-associated genes, such as *Fgfr3* and *Estrogen receptor beta (Esr2)* were upregulated, although not to the level of statistical significance. In contrast, *Htra1* downregulated inhibitors of osteogenesis, such as *Sost*, *Calca*,

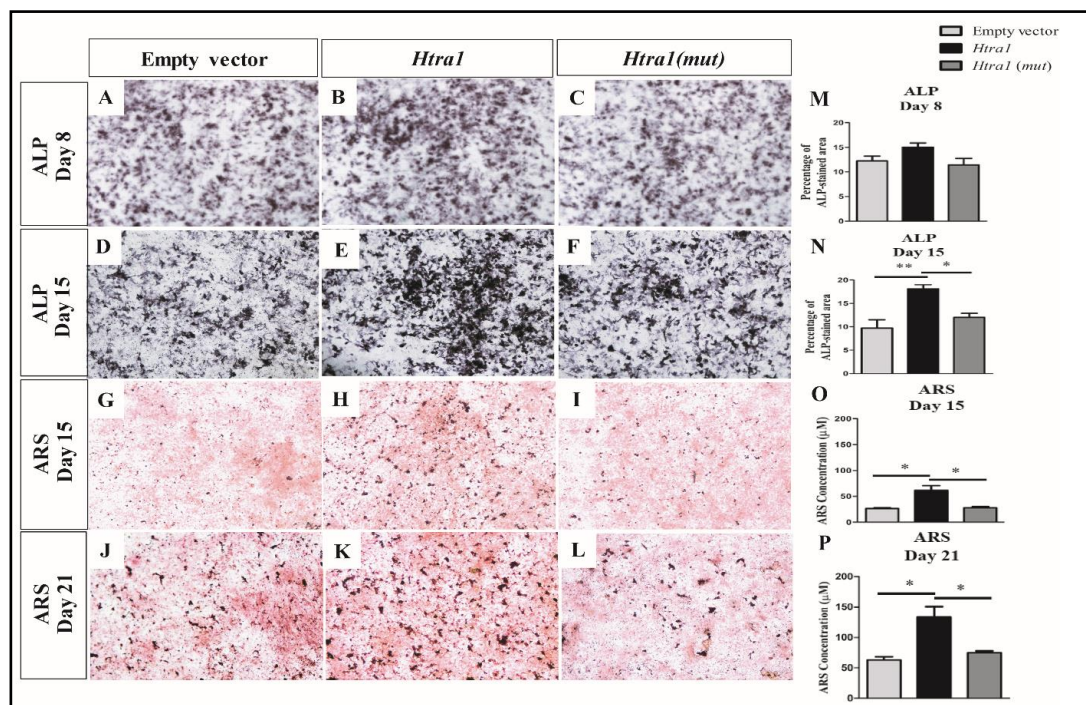


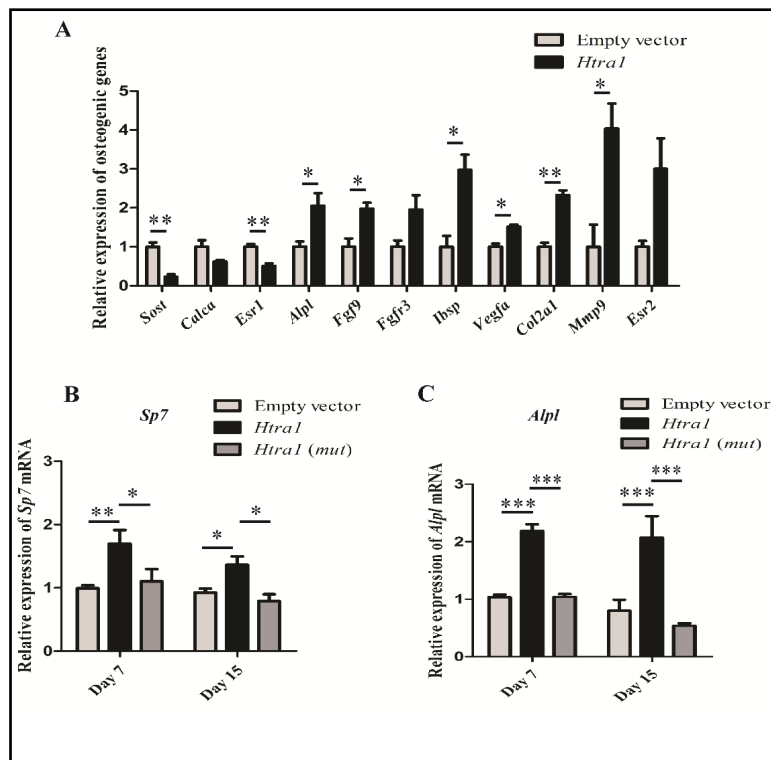
**Fig. 2.** *Htra1* promotes osteogenic differentiation of primary mesenchymal progenitor cells. (A-F) Representative images of ALP staining in primary mesenchymal progenitor cells transfected with empty vector (A and D), *Htra1* (B and E), and *Htra1 (mut)* expression vectors (C and F) at d8 (A-C) and d15 (D-F) of osteoblast differentiation. Overexpression of *Htra1* resulted in an increase in ALP staining at d15, compared to the empty vector- and *Htra1 (mut)*-transfected cells (D-F). (G-L) Representative images of ARS staining in primary mesenchymal progenitor cells transfected with empty vector (G and J), *Htra1* (H and K), and *Htra1 (mut)* (I and L) expression vectors at d15 (G-I) and d21 (J-L). ARS staining revealed an increase in mineralized matrix in *Htra1*-overexpressed cells, compared to cells treated with empty vector or *Htra1 (mut)* at both d15 and d21 (G-L). ALP-stained percentage area was quantified by ImageJ analyses at d8 (M) and d15 (N). Data are represented as mean ± S.E.M.; one-way ANOVA with Bonferroni posthoc test; \*,  $p < 0.05$ ; \*\*,  $p < 0.01$  ( $n = 4$  biological replicates). Quantitation of ARS-stained osteoblast matrix after overexpression of *Htra1* ( $n = 3$  biological replicates) revealed a significant increase in the amount of bone matrix in *Htra1*-overexpressed cells at d15 (O) and d21 (P), compared to both empty vector- and *Htra1 (mut)*-transfected cells. Data are represented as mean ± S.E.M.; one-way ANOVA with Bonferroni posthoc test; \*,  $p < 0.05$ . Scale bar = 100  $\mu\text{m}$ .

and *Estrogen receptor alpha (Esr1)* 0.23, 0.60, and 0.51-fold, respectively, although *Calca* reduction was not statistically significant (Fig. 3A). Upregulation of the osteoblast markers *Sp7* and *Alpl* by *Htra1* was demonstrated using qPCR. Compared to empty vector-transfected cells, overexpression of *Htra1* significantly upregulated *Sp7* (1.7-fold at d7 and 1.37-fold at d15) and *Alpl* (2.1-fold at both d7 and d15) (Fig. 3B, C). In contrast, the *Htra1 (mut)* vector failed to upregulate the expression of *Sp7* and *Alpl* at d7 and d15 (Fig. 3B, C). These data indicated that *Htra1* regulates several osteogenesis-related genes to promote osteoblast differentiation and that mutation of the protease domain of HTRA1 blocks this activity.

*RUNX2 interacts with the Htra1 promoter to induce Htra1 expression during osteoblast differentiation*

Although *Htra1* overexpression upregulated some osteoblast markers, such as *Alpl* and *Sp7*, *Runx2* was not altered (data not shown). Since RUNX2 and HTRA1 are co-expressed during osteogenesis *in vivo* (Fig. 1), *Runx2* might be upstream of *Htra1* during osteoblast differentiation. To investigate this, *Runx2* was overexpressed in primary mesenchymal progenitor cells for eight days (Fig. 4A). Overexpression of *Runx2* increased the expression of *Htra1* to the same extent as *Sp7* (1.51-fold; Fig. 4B, C), a known transcriptional target of *Runx2* [9, 45]. In addition, the upregulation of *Runx2* resulted in a corresponding increase in RUNX2 (1.91-fold; Fig. 4D, E; Supplementary Fig. 2A) and HTRA1 (2.23-fold; Fig. 4F, G; Supplementary Fig. 2B) protein levels, compared to cells transfected with empty vector. These data show that *Runx2* can induce *Htra1* and HTRA1 expression during osteogenic differentiation. Supporting the idea that RUNX2 regulates *Htra1* directly, several putative

**Fig. 3.** Htra1 regulates the expression of osteogenesis-related genes during differentiation of primary mesenchymal progenitor cells. Osteogenesis gene expression array was carried out at d7 in primary mesenchymal progenitor cells transfected with empty vector or Htra1 overexpression vector during osteogenic differentiation. Differentially expressed genes between the empty vector and Htra1-overexpressing osteoblasts are plotted in the bar graph (A; n=3 biological replicates). Data were normalized to Gapdh Ct values of the respective samples; mean ± S.E.M; Two-tailed unpaired T-test was carried out for each gene separately and represented relative to respective empty vector transfected cells. Relative mRNA expression of osteoblast markers *Sp7* (Osx) (B) and *Alpl* (C) at d7 and d15 in primary mesenchymal progenitor cells after overexpression of Htra1. Compared to empty vector-transfected cells and Htra1 (mut)-transfected cells, overexpression of Htra1 significantly upregulated the gene expression of *Sp7* and *Alpl* at d7 and at d15 (B and C). Data were normalized to 18s rRNA (n=4 biological replicates; mean ± S.E.M; one-way ANOVA with Bonferroni posthoc test, \*, p<0.05; \*\*, p<0.01; \*\*\*, p<0.001) and represented relative to cells transfected with empty vector.



transfected cells. Relative mRNA expression of osteoblast markers *Sp7* (Osx) (B) and *Alpl* (C) at d7 and d15 in primary mesenchymal progenitor cells after overexpression of Htra1. Compared to empty vector-transfected cells and Htra1 (mut)-transfected cells, overexpression of Htra1 significantly upregulated the gene expression of *Sp7* and *Alpl* at d7 and at d15 (B and C). Data were normalized to 18s rRNA (n=4 biological replicates; mean ± S.E.M; one-way ANOVA with Bonferroni posthoc test, \*, p<0.05; \*\*, p<0.01; \*\*\*, p<0.001) and represented relative to cells transfected with empty vector.

RUNX2 binding sites were identified in the genomic region 1kb upstream of the *Htra1* transcriptional start site (Fig. 5A). To examine if RUNX2 binds to this proximal *Htra1* promoter, streptavidin pull-downs were carried out using biotinylated promoter regions of *Htra1* on lysates of d5 differentiating cells. Indeed, RUNX2 protein interacted with both 1 kb (-994 bp to +72 bp) and 0.4 kb (-399 bp to +72 bp) *Htra1* promoter regions (Fig. 5B; Supplementary Fig. 3A, B). In addition, ChIP analyses confirmed that RUNX2 interacts with the proximal 0.4 kb *Htra1* promoter during osteogenic differentiation (Fig. 5C).

To identify more discrete regions of the *Htra1* promoter through which *Runx2* could promote *Htra1* expression, five different regions of the *Htra1* promoter were cloned into a luciferase reporter vector: (i) -994 to +72 bp; (ii) -399 to +72 bp; (iii) -811 to -439 bp; (iv) -295 to +72 bp; and (v) -199 to +72 (Fig. 6A). Constructs were transfected individually into primary mesenchymal progenitor cells along with either a *Runx2* overexpression or an empty vector. Dual luciferase reporter assay was carried out 48 h after transfection. Overexpression of *Runx2* significantly increased luciferase activity of all the *Htra1* promoter constructs except the -811 to -439 bp construct (Fig. 6B). Specifically, *Runx2* increased expression of the proximal *Htra1* promoter fragments -994 to +72 bp, -295 to +72 bp, and -199 to +72 bp by 146%, 145%, and 134%, respectively, with the -399 to +72 bp fragment showing the greatest increase in expression to 192% compared to control (empty vector) levels. These results highlighted the importance of *Htra1* promoter fragments that contained putative RUNX2 binding site(s) between -399 to +72 bp in order for *Runx2* to induce *Htra1* expression during osteoblast differentiation of mesenchymal cells.

**Fig. 4.** RUNX2 promotes the expression of *Htra1* in primary mesenchymal progenitor cells (A-C) Relative mRNA expression of *Runx2* (A), *Htra1* (B), and *Sp7* (C) at d8 during osteogenic differentiation of primary mesenchymal progenitor cells after overexpression of *Runx2*. (D-G) Western blot analyses of RUNX2 (D, E) and HTRA1 (F, G) at d8 during osteogenic differentiation of primary mesenchymal progenitor cells after overexpression of *Runx2*. Immunoblots (D and F) and densitometric analyses (E and G) show increase in RUNX2 and HTRA1 protein with the overexpression of *Runx2*. Densitometry data (n=3 biological replicates) were normalized to  $\beta$ -ACTIN and represented relative to empty vector control (mean $\pm$ S.E.M; Two-tailed unpaired T-test, \*p<0.05, \*\*p<0.01; \*\*\*p<0.001).

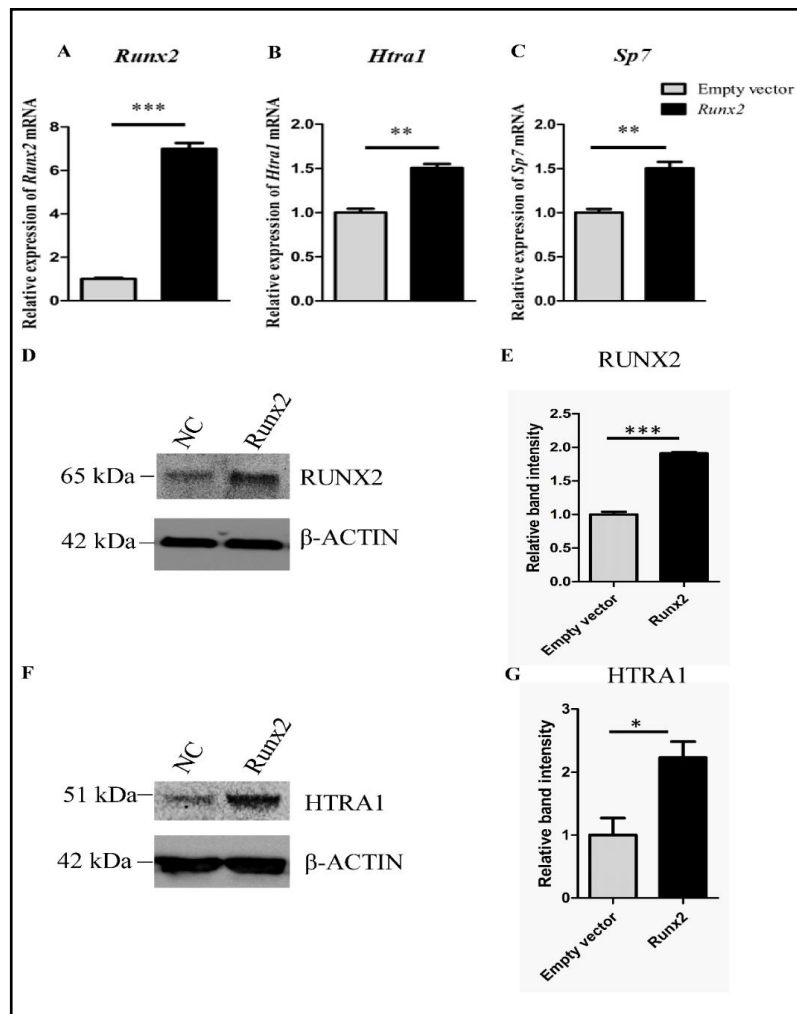
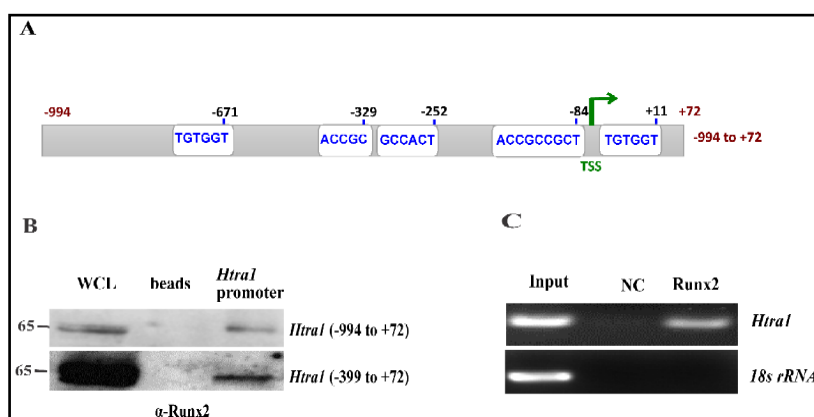


**Fig. 5.** RUNX2 interacts with the Htra1 proximal promoter in primary mesenchymal progenitor cells. (A) Schematic diagram showing the promoter region of Htra1 (-994 bp to +200 bp) with putative RUNX2 binding sites. RCCRC is the known RUNX2 consensus binding site and TGTGGT is the reverse complement of ACCACA (RCCRC). Streptavidin-agarose pull-down assay (B) reveals the interaction of RUNX2 with biotinylated Htra1 promoter probes of length 1 kb (-994 to +72) (upper panel) and proximal 0.4 kb (-399 to +72 bp) (lower panel). (C) ChIP assay was performed in differentiating primary mesenchymal progenitor cells during osteoblast differentiation at d5. ChIP assay confirms the interaction of RUNX2 protein with the proximal Htra1 promoter during osteoblast differentiation (C). TSS, transcription start site; NC, negative control IgG; WCL, whole cell lysate.



To identify critical RUNX2 binding sites for *Htra1* promoter activity, putative RUNX2 binding sites on the -399 to +72 bp proximal *Htra1* promoter fragment were mutated and *Runx2*-mediated expression was analyzed. The specific RUNX2 binding sites mutated were at -252 bp (Mut1), -84 bp (Mut2), and +11 bp (Mut3), alone or in combination (Fig. 7A). Overexpression of *Runx2* increased the *Htra1* promoter activity of wild-type (-399 to +72 bp) and Mut3 (+11 bp) to 165% and 151%, respectively (Fig. 7B), suggesting that the putative RUNX2 binding site at +11 bp was not required for *Runx2* activation. However, Mut1 (-252 bp) and Mut2 (-84 bp) constructs, alone or in combination, blocked *Runx2*-mediated promoter activity of *Htra1* (Fig. 6B), suggesting that both of these sites are required for *Runx2* activation. Specifically, the *Runx2*-mediated expression levels of the Mut1 and Mut2 proximal *Htra1* promoter regions were 95% and 104%, respectively, of control values (Fig. 7B). Combined proximal *Htra1* promoter region mutations (Mut1\**Mut2*) also failed to increase expression by *Runx2* (75%). To confirm that binding of RUNX2 to the -252 bp and -84 bp sites is required for *Runx2* activation of the *Htra1* promoter, streptavidin pull-down assays were performed using either the biotinylated wild-type *Htra1* promoter probes (-399 to +72 bp) or the Mut1, Mut2, or Mut3 probes of the same region. Western blot analysis showed that RUNX2 was able to bind to the wild-type and Mut3 probes in differentiating osteoblasts (Fig. 7C; Supplementary Fig. 3C). In contrast, RUNX2 did not bind to Mut1 or Mut2 probes (Fig. 7C). These data showed that *Runx2* induces *Htra1* expression during osteoblast differentiation via RUNX2 binding to sites -252 bp and -84 bp at the proximal *Htra1* promoter.

## Discussion

Despite considerable knowledge of the signalling mechanisms governing osteoblast differentiation, several interacting partners and their role in osteogenesis remain obscure. In this study, we demonstrated that the serine protease *Htra1* promotes osteoblast differentiation of primary mesenchymal progenitor cells. In addition, we revealed a specific molecular interaction between RUNX2 and *Htra1* during osteoblast differentiation, delineating that RUNX2 binds to the proximal *Htra1* promoter to activate *Htra1* expression. Our data significantly improve the understanding of the role of *Htra1* in osteoblast differentiation and unravel a novel interaction between *Htra1* and *Runx2*.

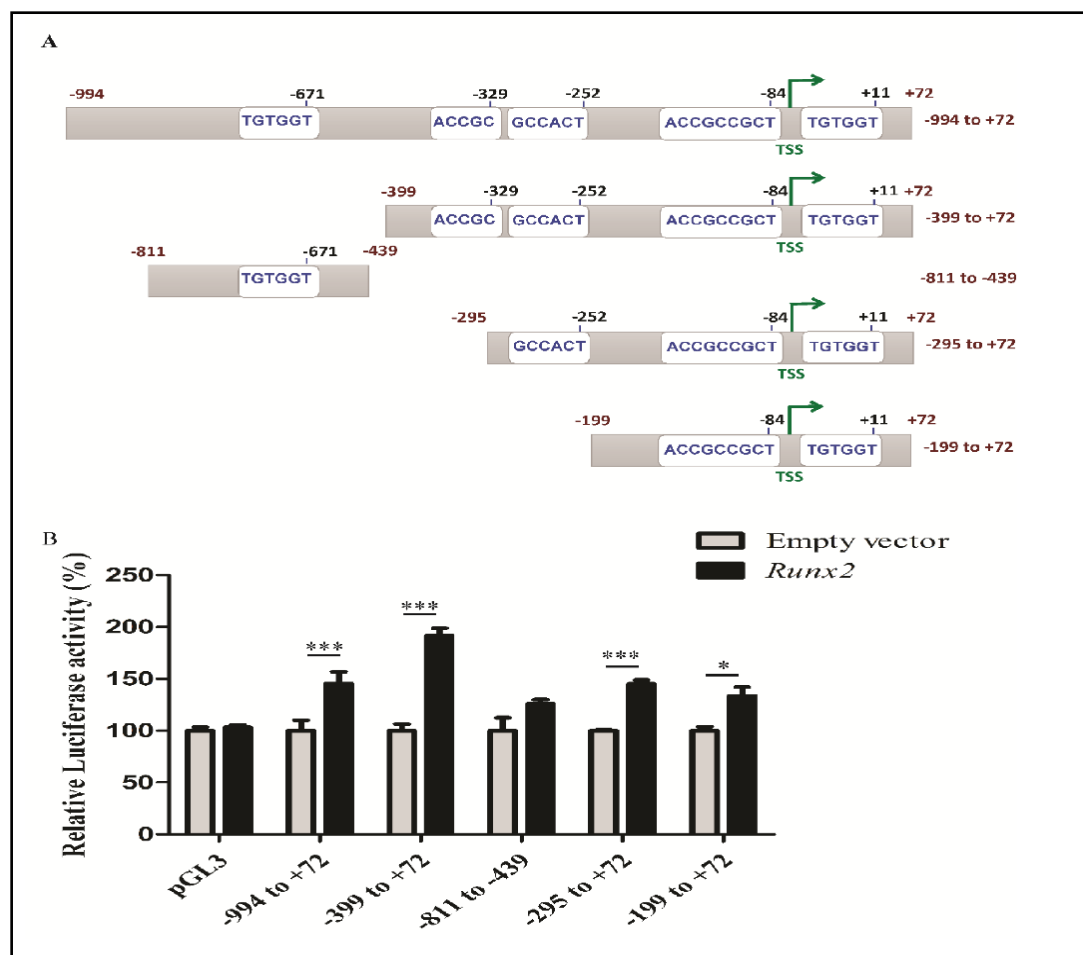


**Fig. 6.** RUNX2 activates the proximal Htra1 promoter. (A) Schematics showing five different lengths of Htra1 promoter fragments cloned into pGL3 promoter luciferase vector. (B) Relative luciferase activity of the Htra1 promoter fragments 48h after transfection with Runx2 overexpression vector in primary mesenchymal progenitor cells. RUNX2 significantly increased the luciferase activity of all the Htra1 promoter constructs except the -811 to -439 bp construct. Data were normalized to respective empty vector-transfected cells and represented as percentage activity. Mean  $\pm$  S.E.M; two-way ANOVA with Bonferroni posthoc test; \*,  $p < 0.05$ ; \*\*\*,  $p < 0.001$ .

Conflicting reports on whether *Htra1* promotes or inhibits osteoblast differentiation might relate to the specific progenitor cell or the culture conditions in which an osteogenic role for *Htra1* was evaluated. Here, the co-expression of HTRA1 and RUNX2 in developing craniofacial bones led to the hypothesis that *Runx2*-mediated *Htra1* expression regulates osteoblast differentiation of craniofacial mesenchymal progenitor cells. Supporting this hypothesis, *Htra1* overexpression in primary craniofacial mesenchymal progenitor cells enhanced osteogenic marker expression and secretion of mineralized bone matrix. As such, these findings are consistent with the reported osteoblast-promoting role of HTRA1 in human bone marrow-derived stem cells [20], mouse adipose-derived stromal cells [22], and periodontal ligament cells [46]. Conversely, *Htra1* was reported to be an inhibitor of matrix mineralization in murine 2T3 and KusaO cell lines [23, 24]. These cell lines, however, were transformed with SV40, which significantly reduces the expression of *Htra1* [47], thus complicating analyses of the role of *Htra1* in osteoblast differentiation [20, 48]. In addition, these studies investigated the role of *Htra1* after stimulation with BMP2 [23, 24]. Even though the addition of BMP2 can upregulate *Htra1* in C2C12 preosteoblasts [49], a potential role for *Htra1* in osteoblast differentiation might have been overwhelmed by BMP pathway

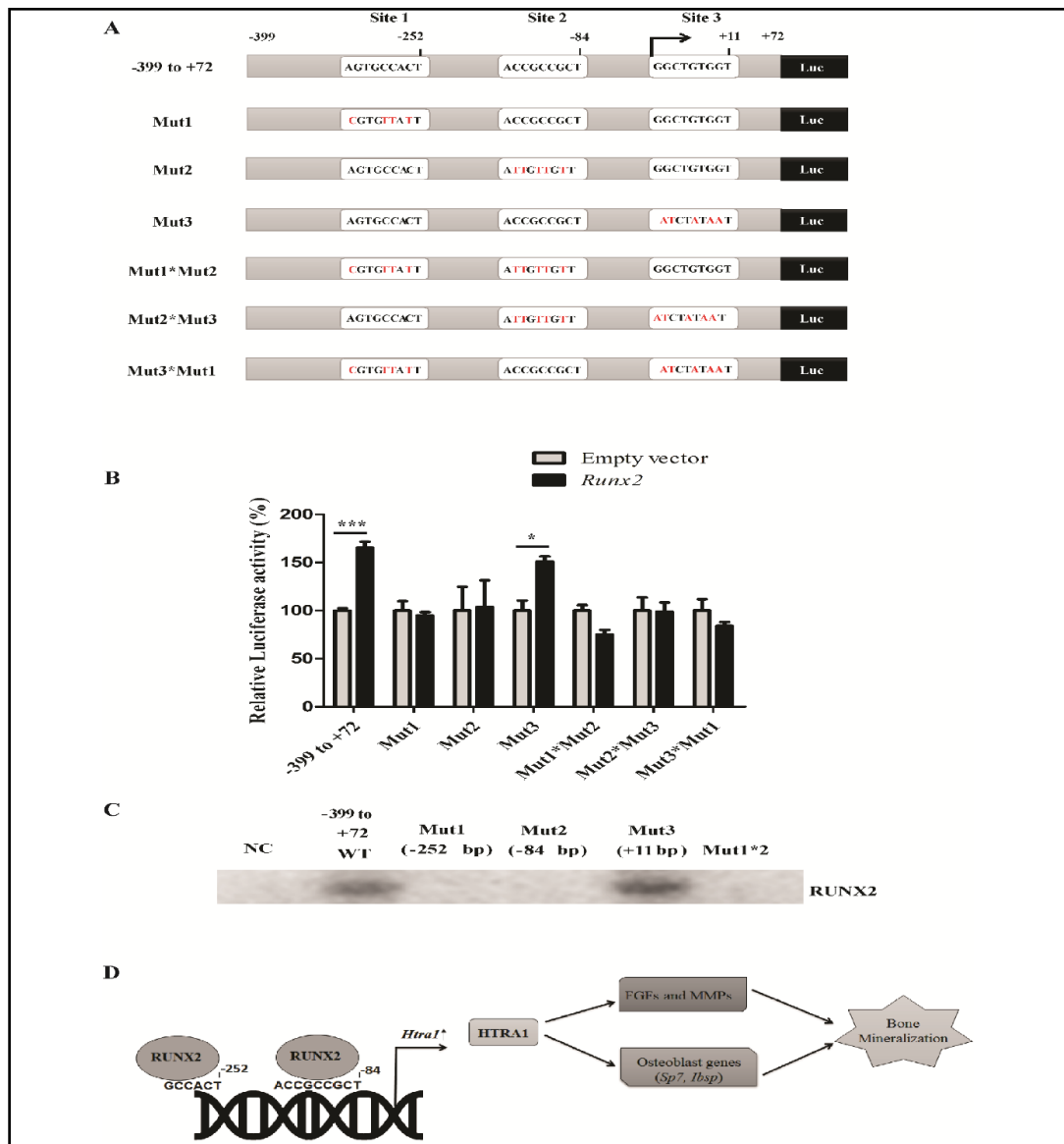


**Fig. 7.** Mutation of putative RUNX2 binding sites at -252 bp and -84 bp in the Htra1 proximal promoter abrogates the activation of Htra1 by Runx2. (A) Schematics diagram showing three putative RUNX2 binding sites on the 0.4 kb Htra1 promoter (-399 to +72 bp) and site-directed mutagenesis of putative binding sites at -252 bp (Mut1), -84 bp (Mut2) and +11 bp (Mut3) alone or in combination in the Htra1 promoter. (B) Relative luciferase activity of wild-type and mutated Htra1 promoter fragments (-399 to +72 bp) after overexpression of Runx2. Runx2 promotes the luciferase activity of the wild-type Htra1 promoter (-399 to +72 bp) and promoter construct with mutation of the site 3 at +11 bp (Mut3), whereas it failed to induce luciferase activity of the Htra1 promoter constructs with mutation of binding site 1 (Mut1) or site 2 (Mut2) alone or in combination. Relative luciferase activity was normalized to empty vector and represented as percentage activity. Mean  $\pm$  S.E.M; two-way ANOVA with Bonferroni posthoc test; \*,  $p < 0.05$ ; \*\*\*,  $p < 0.001$ . Streptavidin-agarose pull-down assay (C) showing the interaction of RUNX2 with biotinylated wild-type Htra1 promoter probe (-399 to +72 bp) and mutated probes of site +11 bp (Mut3), however, RUNX2 failed to bind to mutated probes of sites -252 bp (Mut1) or -84 bp (Mut2). (D) Schematics showing the role of Htra1 in osteogenic differentiation. RUNX2 binds to two binding sites at -252 bp and -84 bp in the proximal Htra1 promoter to induce Htra1 mRNA expression in primary mesenchymal osteoprogenitor cells. Htra1 induces FGF pathway-related genes and Mmp's as well as osteoblast genes, such as Sp7 and Ibsp, to promote bone matrix mineralization.

stimulation, a dominant inducer of osteogenesis. Here, we have used a gain of function approach to show that *Htra1* induces osteogenic differentiation of the mesenchymal progenitor cells. A caveat from the current study is the lack of complementary loss of function approach to check if silencing *Htra1* inhibits osteogenic differentiation. However, it is known from the literature that silencing of *Runx2* during osteogenic differentiation using *Runx2* shRNA downregulates *Htra1* expression, in addition to several known RUNX2-responsive genes such as *Alpl*, *Mmp13* and *Ibsp* [11]. *Htra1* deficient mice exhibit no obvious alteration in bone phenotype *in vivo* [48], but other HTRA members might compensate for *Htra1* function. HTRA3, which shares the highest homology with HTRA1, is also expressed during bone formation [18, 48]. The role of *Htra3* in osteoblast differentiation is unknown, but *Htra1* and *Htra3* could be functionally redundant in mediating osteogenesis of mesenchymal stem cells.

Regarding the influence of RUNX2 in regulating the expression of other Htra family members, Wu et al. (2014) show that *Htra1* is the only Htra family member in the list of RUNX2-responsive genes during osteogenic differentiation in an unbiased microarray approach [11]. In addition, among the *Htra* family members, *Htra1* alone is noted as RUNX2-responsive in bone metastatic prostate cancer cells [50]. RUNX2 does bind to the genomic regions of *Htra1*, *Htra3*, and *Htra4* during osteogenic differentiation, but RUNX2 only binds to the promoter region of *Htra1*, while it binds to introns or exons for *Htra3* and *Htra4* [11]. In fact, most RUNX2-responsive genes exhibit binding sites in the promoter region, rather than introns or exons [6, 8-9, 11]. In this study, we delineated the molecular interactions of RUNX2 at two specific sites in the *Htra1* promoter that seem to regulate *Htra1* expression during osteoblast differentiation. Other members of the Htra family, including *Htra3* and *Htra4*, do not seem to be RUNX2-responsive, but might function redundantly through different genetic networks that impact bone differentiation. Further work is needed to decipher the role and mechanism involving these Htra family members in an osteoblast-specific compound mutant mice model.

Through what downstream pathways might *Htra1* promote osteoblast differentiation of mesenchymal progenitor cells? Osteogenic gene expression analysis performed here revealed that *Htra1* upregulated the FGF signalling genes *Fgf9* and *Fgfr3*, and FGF signalling promotes osteogenesis [51]. In addition, HTRA1 proteolytic cleavage of ECM proteins such as Biglycan, Syndecan-4, and Glypican-4 promotes long-range FGF signalling in *Xenopus* embryos [28]. In turn, FGF signalling is necessary and sufficient for *Htra1* expression in chick facial and forelimb mesenchyme [31]. HTRA1 induces adipogenesis via MAP kinase-dependent MMP production in human mesenchymal stem cells [21]. In our study, the induction of *Mmp9* expression by *Htra1* might be related to the demonstrated upregulation of MMPs by HTRA1 proteolytic cleavage of ECM proteins, such as Fibronectin [21, 27] [25]. Therefore, a FGF-Runx2-Htra1-MMP signalling network could be vital in osteoblast differentiation (Fig. 7D).

Other genes identified here to be downstream of *Htra1* during osteoblast differentiation have known osteogenic roles. *IBSP* expression increased after HTRA1 overexpression in human bone marrow-derived mesenchymal stem cells [20]. HTRA1 and IBSP co-localize during bone regeneration in osteo-induced spheroid cultures, where HTRA1 is hypothesized to fragment IBSP for proper matrix mineralization [20]. This might provide a mechanism for *Htra1*-induced matrix mineralization in primary craniofacial mesenchymal cells reported here. Also, we found that *Htra1* overexpression downregulated *Sost*, *Calca*, and *Esr1*. *Sost* is an antagonist of WNT signalling and is a negative regulator of bone formation [52], and *SOST* was previously reported to be inhibited by HTRA1 during osteoblast differentiation of human bone marrow-derived mesenchymal stem cells [20].

Regarding critical upstream regulators of *Htra1* during osteoblast differentiation, we showed that RUNX2 is recruited to the proximal *Htra1* promoter to activate *Htra1* expression. *Runx2* plays a critical role in chondrocyte maturation and bone formation [1]. RUNX2 binds to RUNT binding site RCCRC(A/T) [10] in the promoter regions of downstream genes to drive osteoblast-specific expression [5, 53, 54]. Several targets of RUNX2 during osteogenesis are not yet functionally characterized [11]. Recently, ChIP-seq analysis of RUNX2 during

osteoblast differentiation identified several putative target genes, including *Htra1* [11]. Since false-positives from ChIP-seq analysis are generally unavoidable, characterization of putative downstream targets is essential. In our study, RUNX2 was demonstrated by multiple binding and reporter assays to interact with the proximal -399 to +72 bp region of the *Htra1* promoter to promote *Htra1* expression during osteoblast differentiation. Furthermore, mutation analyses revealed two RUNX2 binding sites (-252 bp and -84 bp) required for the activation of *Htra1* osteogenic expression. The proximity of these binding sites to the transcription start site is comparable to the promoter interaction of RUNX2 with many other target genes, such as *Col10a1* [55], *Ibsp* [56], and *Mmp9* [57]. As such, the data here uncovers a previously unknown functional interaction between RUNX2 and *Htra1*.

The functional interaction of RUNX2 and *Htra1* might be important in several pathological conditions, including cancer. *Runx2* is a negative regulator of cell proliferation, and suppression of *Runx2* expression is linked to tumorigenesis [58, 59]. Moreover, forced expression of *Runx2* inhibits osteosarcoma cell proliferation [60]. *Htra1* is also a tumor suppressor gene, inhibiting cancer cell proliferation [61, 62]. Therefore, considering the role of *Htra1* as a tumor suppressor and modulator of MMP expression, the regulation of *Htra1* by *Runx2* identified here in osteoblasts might have physiological and pathological relevance in other cell lineages. Further studies are needed to address the interaction of RUNX2 and *Htra1* in other systems, such as tumorigenesis.

## Conclusion

In conclusion, our data show that *Htra1* is a novel direct downstream target of RUNX2, which binds to the *Htra1* promoter at -252 bp and -84 bp, and *Htra1* promotes osteoblast differentiation of primary mesenchymal progenitor cells.

## Acknowledgements

This work was supported by Discovery Grant 171317-2012 to AJN from the Natural Sciences and Engineering Research Council of Canada (NSERC) and, in part, by a Subtelny Orthodontic Clinical Research Grant from American Cleft Palate-Craniofacial Association (ACPA-CPF), USA to PPRI and a Canadian Institute for Health Research grant 148683 to BFE.

PPRI was a recipient of the Apotex Graduate Scholarship Award from the College of Pharmacy and Nutrition, University of Saskatchewan; Graduate Research fellowship and Saskatchewan Innovation and Opportunity Scholarships from the College of Graduate Studies and Research, University of Saskatchewan. MPT was a recipient of the Dean's Graduate Scholarship, University of Saskatchewan and an endMS Doctoral Studentship award from the Multiple Sclerosis Society of Canada (MSSC). The authors acknowledge Larhonda Sobchishin for providing technical expertise and Rongqi Liu and Nasim Rostampour for technical assistance.

The protocol for the use of animals was approved by the University of Saskatchewan's Animal Research Ethics Board and adhered to the Canadian Council on Animal Care guidelines for humane animal use.

## Author contributions

PPRI, BFE and AJN conceived the study. AJN coordinated the study. PPRI designed, performed all the experiments, analyzed the data and wrote the manuscript. PPRI and MPT performed the luciferase assay and the osteogenesis array experiments. BFE and MPT proofed and revised the manuscript for critical content and interpretation of data and approved the final version for submission.

This manuscript is dedicated to the memory of Dr. Adil J. Nazarali, who passed away before the submission of the manuscript.

## Disclosure Statement

The authors declare no conflicts of interest.

## References

- 1 Komori T, Yagi H, Nomura S, Yamaguchi A, Sasaki K, Deguchi K, Shimizu Y, Bronson RT, Gao YH, Inada M, Sato M, Okamoto R, Kitamura Y, Yoshiki S, Kishimoto T: Targeted disruption of Cbfa1 results in a complete lack of bone formation owing to maturational arrest of osteoblasts. *Cell* 1997;89:755–764.
- 2 Lee B, Thirunavukkarasu K, Zhou L, Pastore L, Baldini A, Hecht J, Geoffroy V, Ducy P, Karsenty G: Missense mutations abolishing DNA binding of the osteoblast-specific transcription factor OSF2/CBFA1 in cleidocranial dysplasia. *Nat Genet* 1997;16:307–310.
- 3 Otto F, Kanegane H, Mundlos S: Mutations in the RUNX2 gene in patients with cleidocranial dysplasia. *Hum Mutat* 2002;19:209–216.
- 4 Jaruga A, Hordyjewska E, Kandzierski G, Tylzanowski P: Cleidocranial dysplasia and RUNX2-clinical phenotype–genotype correlation. *Clin Genet* 2016;90:393–402.
- 5 Roca H, Phimpilai M, Gopalakrishnan R, Xiao G, Franceschi RT: Cooperative interactions between RUNX2 and homeodomain protein-binding sites are critical for the osteoblast-specific expression of the bone sialoprotein gene. *J Biol Chem* 2005;280:30845–30855.
- 6 Jiménez MJ, Balbín M, López JM, Alvarez J, Komori T, López-Otín C: Collagenase 3 is a target of Cbfa1, a transcription factor of the runt gene family involved in bone formation. *Mol Cell Biol* 1999;19:4431–4442.
- 7 Wang X, Manner PA, Horner A, Shum L, Tuan RS, Nuckolls GH: Regulation of MMP-13 expression by RUNX2 and FGF2 in osteoarthritic cartilage. *Osteoarthritis Cartilage* 2004;12:963–973.
- 8 Nakashima K, Zhou X, Kunkel G, Zhang Z, Deng JM, Behringer RR, de Crombrughe B: The novel zinc finger-containing transcription factor osterix is required for osteoblast differentiation and bone formation. *Cell* 2002;108:17–29.
- 9 Nishio Y, Dong Y, Paris M, O’Keefe RJ, Schwarz EM, Drissi H: Runx2-mediated regulation of the zinc finger Osterix/Sp7 gene. *Gene* 2006;372:62–70.
- 10 Kamachi Y, Ogawa E, Asano M, Ishida S, Murakami Y, Satake M, Ito Y, Shigesada K: Purification of a mouse nuclear factor that binds to both the A and B cores of the polyomavirus enhancer. *J Virol* 1990;64:4808–4819.
- 11 Wu H, Whitfield TW, Gordon JA, Dobson JR, Tai PW, van Wijnen AJ, Stein JL, Stein GS, Lian JB: Genomic occupancy of Runx2 with global expression profiling identifies a novel dimension to control of osteoblastogenesis. *Genome Biol* 2014;15:R52.
- 12 Yang Z, Camp NJ, Sun H, Tong Z, Gibbs D, Cameron DJ, Chen H, Zhao Y, Pearson E, Li X, Chien J, Dewan A, Harmon J, Bernstein PS, Shridhar V, Zabriskie NA, Hoh J, Howes K, Zhang K: A variant of the HTRA1 gene increases susceptibility to age-related macular degeneration. *Science* 2006;314:992–993.
- 13 Hara K, Shiga A, Fukutake T, Nozaki H, Miyashita A, Yokoseki A, Kawata H, Koyama A, Arima K, Takahashi T, Ikeda M, Shiota H, Tamura M, Shimoe Y, Hirayama M, Arisato T, Yanagawa S, Tanaka A, Nakano I, Ikeda S, et al.: Association of HTRA1 mutations and familial ischemic cerebral small-vessel disease. *N Engl J Med* 2009;360:1729–1739.
- 14 Mendioroz M, Fernández-Cadenas I, Del Río-Espinola A, Rovira A, Solé E, Fernández-Figueras MT, García-Patos V, Sastre-Garriga J, Domingues-Montanari S, Alvarez-Sabín J, Montaner J: A missense HTRA1 mutation expands CARASIL syndrome to the Caucasian population. *Neurology* 2010;75:2033–2035.
- 15 Beaufort N, Scharrer E, Lux V, Ehrmann M, Huber R, Houlden H, Werring D, Haffner C, Dichgans M: Cerebral small vessel disease-related protease Htra1 processes latent TGF- $\beta$  binding protein 1 and facilitates TGF- $\beta$  signaling. *Proc Natl Acad Sci U S A* 2014;111:16496–16501.
- 16 Chien J, Staub J, Hu SJ, Erickson-johnson MR, Couch FJ, Smith DI, Crawl RM, Kaufmann SH, Shridhar V: A candidate tumor suppressor Htra1 is downregulated in ovarian cancer. *Oncogene* 2004;1636–1644.
- 17 He X, Ota T, Liu P, Su C, Chien J, Shridhar V: Downregulation of Htra1 promotes resistance to anoikis and peritoneal dissemination of ovarian cancer cells. *Cancer Res* 2010;70:3109–3118.
- 18 Tocharus J, Tsuchiya A, Kajikawa M, Ueta Y, Oka C, Kawaichi M: Developmentally regulated expression of mouse Htra3 and its role as an inhibitor of TGF-beta signaling. *Dev Growth Differ* 2004;46:257–274.

- 19 Tsuchiya A, Yano M, Tocharus J, Kojima H, Fukumoto M, Kawaichi M, Oka C: Expression of mouse Htra1 serine protease in normal bone and cartilage and its upregulation in joint cartilage damaged by experimental arthritis. *Bone* 2005;37:323–336.
- 20 Tiaden AN, Breiden M, Mirsaidi A, Weber FA, Bahrenberg G, Glanz S, Cinelli P, Ehrmann M, Richards PJ: Human serine protease HTRA1 positively regulates osteogenesis of human bone marrow-derived mesenchymal stem cells and mineralization of differentiating bone-forming cells through the modulation of extracellular matrix protein. *Stem Cells* 2012;30:2271–2282.
- 21 Tiaden AN, Bahrenberg G, Mirsaidi A, Glanz S, Blüher M, Richards PJ: Novel function of serine protease HTRA1 in inhibiting adipogenic differentiation of human mesenchymal stem cells via MAP Kinase-mediated MMP upregulation. *Stem Cells* 2016;34:1601–1614.
- 22 Glanz S, Filliat G, Mirsaidi A, Tiaden N, Richards PJ: Loss-of-function of Htra1 abrogates all-trans retinoic acid-induced osteogenic differentiation of mouse adipose-derived stromal cells through deficiencies in p70S6K activation. *Stem Cells Dev* 2016;25:687–698.
- 23 Hadfield KD, Rock CF, Inkson CA, Dallas SL, Sudre L, Wallis GA, Boot-Handford RP, Canfield AE: Htra1 inhibits mineral deposition by osteoblasts: requirement for the protease and PDZ domains. *J Biol Chem* 2008;283:5928–5938.
- 24 Wu X, Chim SM, Kuek V, Lim BS, Chow ST, Zhao J, Yang S, Rosen V, Tickner J, Xu J: Htra1 is upregulated during RANKL-induced osteoclastogenesis, and negatively regulates osteoblast differentiation and BMP2-induced Smad1/5/8, ERK and p38 phosphorylation. *FEBS Lett* 2014;588:143–150.
- 25 Vierkotten S, Muether PS, Fauser S: Overexpression of HTRA1 leads to ultrastructural changes in the elastic layer of Bruch's membrane via cleavage of extracellular matrix components. *PLoS One* 2011;6:e22959.
- 26 Grau S, Baldi A, Bussani R, Tian X, Stefanescu R, Przybylski M, Richards P, Jones SA, Shridhar V, Clausen T, Ehrmann M: Implications of the serine protease Htra1 in amyloid precursor protein processing. *Proc Natl Acad Sci U S A* 2005;102:6021–6026.
- 27 Tiaden AN, Klawitter M, Lux V, Mirsaidi A, Bahrenberg G, Glanz S, Quero L, Liebscher T, Wuertz K, Ehrmann M, Richards PJ: Detrimental role for human high temperature requirement serine protease A1 (HTRA1) in the pathogenesis of intervertebral disc (IVD) degeneration. *J Biol Chem* 2012;287:21335–21345.
- 28 Hou S, Maccarana M, Min TH, Strate I, Pera EM: The secreted serine protease xHtra1 stimulates long-range FGF signaling in the early *Xenopus* embryo. *Dev Cell* 2007;13:226–241.
- 29 Hung IH, Yu K, Lavine KJ, Ornitz DM: FGF9 regulates early hypertrophic chondrocyte differentiation and skeletal vascularization in the developing stylopod. *Dev Biol* 2007;307:300–313.
- 30 Behr B, Leucht P, Longaker MT, Quarto N: Fgf-9 is required for angiogenesis and osteogenesis in long bone repair. *Proc Natl Acad Sci U S A* 2010;107:11853–11858.
- 31 Ferrer-Vaquer A, Maurey P, Werzowa J, Firnberg N, Leibbrandt A, Neubüser A: Expression and regulation of HTRA1 during chick and early mouse development. *Dev Dyn* 2008;237:1893–1900.
- 32 Jiang X, Iseki S, Maxson RE, Sucov HM, Morriss-Kay GM: Tissue origins and interactions in the mammalian skull vault. *Dev Biol* 2002;116:106–116.
- 33 Percival CJ, Richtsmeier JT: Angiogenesis and intramembranous osteogenesis. *Dev Dyn* 2013;242:909–922.
- 34 Iyyanar PPR, Nazarali AJ: Hoxa2 inhibits bone morphogenetic protein signaling during osteogenic differentiation of the palatal mesenchyme. *Front Physiol* 2017;8:929.
- 35 Okello DO, Iyyanar PPR, Kulyk WM, Smith TM, Lozanoff S, Ji S, Nazarali AJ: Six2 plays an intrinsic role in regulating proliferation of mesenchymal cells in the developing palate. *Front Physiol* 2017;8:955.
- 36 Iwata J, Tung L, Urata M, Hacia JG, Pelikan R, Suzuki A, Ramenzoni L, Chaudhry O, Parada C, Sanchez-Lara PA, Chai Y: Fibroblast growth factor 9 (FGF9)-pituitary homeobox 2 (PITX2) pathway mediates transforming growth factor  $\beta$  (TGF $\beta$ ) signaling to regulate cell proliferation in palatal mesenchyme during mouse palatogenesis. *J Biol Chem* 2012;287:2353–2363.
- 37 Kwong FN, Richardson SM, Evans CH: Chordin knockdown enhances the osteogenic differentiation of human mesenchymal stem cells. *Arthritis Res Ther* 2008;10:R35.
- 38 Baek JA, Lan Y, Liu H, Maltby KM, Mishina Y, Jiang R: Bmpr1a signaling plays critical roles in palatal shelf growth and palatal bone formation. *Dev Biol* 2011;350:520–531.
- 39 Chiarella E, Aloisio A, Scicchitano S, Lucchino V, Montalcini Y, Galasso O, Greco M, Gasparini G, Mesuraca M, Bond HM, Morrone G: ZNF521 represses osteoblastic differentiation in human adipose-derived stem cells. *Int J Mol Sci* 2018;19:4095.

- 40 Gregory CA, Gunn WG, Peister A, Prockop DJ: An Alizarin red-based assay of mineralization by adherent cells in culture : comparison with cetylpyridinium chloride extraction. *Anal Biochem* 2004;329:77–84.
- 41 Hu SI, Carozza M, Klein M, Nantermet P, Luk D, Crowl RM: Human Htra1, an evolutionarily conserved serine protease identified as a differentially expressed gene product in osteoarthritic cartilage. *J Biol Chem* 1998;273:34406–34412.
- 42 Deng WG, Zhu Y, Montero A, Wu KK: Quantitative analysis of binding of transcription factor complex to biotinylated DNA probe by a streptavidin-agarose pulldown assay. *Anal Biochem* 2003;323:12–18.
- 43 Ji S, Doucette JR, Nazarali AJ: Sirt2 is a novel in vivo downstream target of Nkx 2.2 and enhances oligodendroglial cell differentiation. *J Mol Cell Biol* 2011;3:351–359.
- 44 Thangaraj MP, Furber KL, Gan JK, Ji S, Sobchishin L, Doucette JR, Nazarali AJ: RNA binding protein quaking stabilizes Sirt2 mRNA during oligodendroglial differentiation. *J Biol Chem* 2017;292:5166–5182.
- 45 Nakashima K, Zhou X, Kunkel G, Zhang Z, Deng JM, Behringer RR, de Crombrughe B: The novel zinc finger-containing transcription factor osterix is required for osteoblast differentiation and bone formation. *Cell* 2002;108:17–29.
- 46 Li R, Zhang Q: Htra1 may regulate the osteogenic differentiation of human periodontal ligament cells by TGF- $\beta$ 1. *J Mol Histol* 2015;46:137–144.
- 47 Zumbunn J, Trueb B: Primary structure of a putative serine protease specific for IGF-binding proteins. *FEBS Lett* 1996;398:187–192.
- 48 Filliat G, Mirsaidi A, Tiaden AN, Kuhn GA, Weber FE, Oka C, Richards PJ: Role of HTRA1 in bone formation and regeneration : In vitro and in vivo evaluation. *PLoS One* 2017;12:e0181600.
- 49 Bustos-valenzuela JC, Fujita A, Halcsik E, Granjeiro JM, Sogayar MC: Unveiling novel genes upregulated by both rhBMP2 and rhBMP7 during early osteoblastic transdifferentiation of C2C12 cells. *BMC Res Notes* 2011;4:370.
- 50 Baniwal SK, Khalid O, Gabet Y, Shah RR, Purcell DJ, Mav D, Kohn-Gabet AE, Shi Y, Coetzee GA, Frenkel B: Runx2 transcriptome of prostate cancer cells : insights into invasiveness and bone metastasis. *Mol Cancer* 2010;9:258.
- 51 Park OJ, Kim HJ, Woo KM, Baek JH, Ryoo HM: FGF2-activated ERK mitogen-activated protein kinase enhances Runx2 acetylation and stabilization. *J Biol Chem* 2010;285:3568–3574.
- 52 Kamiya N, Kobayashi T, Mochida Y, Yu PB, Yamauchi M, Kronenberg HM, Mishina Y: Wnt inhibitors Dkk1 and Sost are downstream targets of BMP signaling through the type IA receptor (BMPRIA) in osteoblasts. *J Bone Miner Res* 2010;25:200–210.
- 53 Lamour V, Detry C, Sanchez C, Henrotin Y, Castronovo V, Bellahcene A: Runx2- and histone deacetylase 3-mediated repression is relieved in differentiating human osteoblast cells to allow high bone sialoprotein expression. *J Biol Chem* 2007;282:36240–36249.
- 54 Hu R, Liu W, Li H, Yang L, Chen C, Xia ZY, Guo LJ, Xie H, Zhou HD, Wu XP, Luo XH: A Runx2/miR-3960/miR-2861 regulatory feedback loop during mouse osteoblast differentiation. *J Biol Chem* 2011;286:12328–12339.
- 55 Li F, Lu Y, Ding M, Napierala D, Abbassi S, Chen Y, Duan X, Wang S, Lee B, Zheng Q: Runx2 contributes to murine Col10a1 gene regulation through direct interaction with its cis-enhancer. *J Bone Miner Res* 2011;26:2899–2910.
- 56 Roca H, Phimpilai M, Gopalakrishnan R, Xiao G, Franceschi RT: Cooperative interactions between RUNX2 and homeodomain protein-binding sites are critical for the osteoblast-specific expression of the bone sialoprotein gene. *J Biol Chem* 2005;280:30845–30855.
- 57 Pratap J, Javed A, Languino LR, van Wijnen AJ, Stein JL, Stein GS, Lian JB: The Runx2 osteogenic transcription factor regulates matrix metalloproteinase 9 in bone metastatic cancer cells and controls cell invasion. *Mol Cell Biol* 2005;25:8581–8591.
- 58 Kilbey A, Blyth K, Wotton S, Terry A, Jenkins A, Bell M, Hanlon L, Cameron ER, Neil JC: Runx2 disruption promotes immortalization and confers resistance to oncogene-induced senescence in primary murine fibroblasts. *Cancer Res* 2007;67:11263–11271.
- 59 Zaidi SK, Pande S, Pratap J, Gaur T, Grigoriu S, Ali SA, Stein JL, Lian JB, van Wijnen AJ, Stein GS: Runx2 deficiency and defective subnuclear targeting bypass senescence to promote immortalization and tumorigenic potential. *Proc Natl Acad Sci U S A* 2007;104:19861–19866.

- 60 Lucero CM, Vega OA, Osorio MM, Tapia JC, Antonelli M, Stein GS, van Wijnen AJ, Galindo MA: The cancer-related transcription factor Runx2 modulates cell proliferation in human osteosarcoma cell lines. *J Cell Physiol* 2013;228:714–723.
- 61 Baldi A, De Luca A, Morini M, Battista T, Felsani A, Baldi F, Catricalà C, Amantea A, Noonan DM, Albin A, Natali PG, Lombardi D, Paggi MG: The Htra1 serine protease is down-regulated during human melanoma progression and represses growth of metastatic melanoma cells. *Oncogene* 2002;21:6684–6688.
- 62 Chien J, Staub J, Hu SI, Erickson-Johnson MR, Couch FJ, Smith DI, Crowl RM, Kaufmann SH, Shridhar V: A candidate tumor suppressor Htra1 is downregulated in ovarian cancer. *Oncogene* 2004;23:1636–1644.